SYNTHESIS OF A Fe_3O_4/PAA-BASED MAGNETIC FLUID FOR FARADAY-ROTATION MEASUREMENTS

SINTEZA MAGNETNE TEKOČINE NA OSNOVI Fe_3O_4/PAA ZA MERITVE FARADAYEVE ROTACIJE

Serhat Küçükdermenci[1,3], Deniz Kutluay[1,2], İbrahim Avgın[1]

[1]Department of Electrical and Electronics Engineering, Ege University, Bornova 35100, Izmir, Turkey
[2] Departments of Electronics and Communications Engineering, Izmir University, Uckuyular 35290, Izmir, Turkey
[3]Department of Electrical and Electronics Engineering, Balikesir University, Campus of Cagis, 10145 Balikesir, Turkey
serhat.kucukdermenci@ege.edu.tr

Highly water-soluble Fe_3O_4/PAA (polyacrylic acid) nanoparticles (NPs) were synthesized with the high-temperature hydrolysis method. We report the first demonstration of Faraday rotation (FR) for a magnetic fluid (MF) synthesized with this novel method. The experiments were performed in the DC regime ($0–6 \cdot 10^{-2}$ T) at room temperature for 14 concentrations from 1.8 mg/ml to 5 mg/ml. The maximum rotation was recorded as $0.96°$ cm^{-1} for 3.33 mg/ml and this is called the critical concentration ($C_{CRITICAL}$). It was found that the rotation tends to decrease when the concentration is higher than $C_{CRITICAL}$. The MF behavior for FR is discussed with respect to substructure interactions (particle-particle, chain-chain). This work provides a new insight for the FR investigations of MFs including highly water-soluble magnetic NPs.

Keywords: magnetic fluids, Fe_3O_4 nanoparticles, magneto-optic response, Faraday rotation

V vodi dobro topni nanodelci Fe_3O_4/PAA (poly acrylic acid) so bili sintetizirani po metodi visokotemperaturne hidrolize. Poročamo o prvi demonstraciji Faradayeve rotacije (FR) za magnetno raztopino (MF), sintetizirano po tej novi metodi. Preizkusi so bili izvršeni v DC-režimu ($0–6 \cdot 10^{-2}$ T) pri sobni temperaturi za 14 različnih koncentracij od 1,8 mg/ml do 5 mg/ml. Največja rotacija je bila ugotovljena kot $0,96°$ cm^{-1} pri 3,33 mg/ml, kar smo imenovali kritična koncentracija ($C_{CRITICAL}$). Ugotovljeno je bilo, da se rotacija zmanjšuje, če je koncentracija višja od $C_{CRITICAL}$. Lastnost MF za FR je bila obravnavana z interakcijami podstrukture (delec-delec, veriga-veriga). To delo ponuja nov pogled v študij FR magnetnih raztopin (MFs), vključno z v vodi dobro topnimi nanodelci (NPs).

Ključne besede: magnetna tekočina, nanodelci Fe_3O_4, magnetnooptični odgovor, Faradeyeva rotacija

1 INTRODUCTION

Magnetic NPs have unique colloidal, magnetic and optical properties that differ from their bulk counterparts.[1–8] Core-shell NPs have been a topic of great interest due to their potential use in biology[9,10], imaging[11], medicine[12–14] and DNA separation.[15,16] Colloidal suspensions of magnetic NPs can self-assemble into ordered structures. The ability to manipulate this assembly with external tuning parameters such as the field, the temperature and the concentration is essential for developing new stimuli-responsive materials.

MFs, also named ferrofluids, are colloidal suspensions of magnetic NPs that have both characteristics – the fluidity of liquids and the magnetism of solid magnetic materials. Several applications of MFs have recently been introduced, such as a detection system design for glucose concentration in addition to optical-device applications.[17] It is suitable for fabricating optical devices such as optical attenuator, light modulator, optical switch, etc., by using the magneto-optic properties of MFs.[18–20]

In 2007, the Yin group synthesized novel superparamagnetic, magnetite colloidal NPs that can self-assemble into one-dimensional (1D) particle chains and exhibit excellent tunable photonic properties.[21] A suspension of these NPs displays tunable colors in the visible range of the electromagnetic spectrum. The freedom to tune a diffraction color not only depends on the particle size but also varies with the strength of an applied external magnetic field. Since then there has been a widespread interest in these NPs and their applications. Despite their tremendous potential in various applications, interesting fundamental questions referring to their colloidal crystallization with and without a magnetic field remain unanswered. Therefore, we report on the first demonstration of FR for MFs based on these NPs.

FR has been demonstrated in the visible[22,23] NIR[24,25] and MIR[26] regimes for different kinds of ferrofluids. Experimental investigation on γ-Fe_2O_3 NPs FR was done due to the particle-size dependence. Water-based ferrofluid samples are synthesized with the coprecipitation method followed by a size-sorting process[27]. The wavelength and concentration dependence of FR in MFs was studied by Yusuf et al.[28,29] Here we demonstrate that long-term, stable MFs including highly water-soluble NPs show FR in a DC regime ($0–6 \cdot 10^{-2}$ T) at room temperature. Water-based ferrofluid samples are synthesized with a novel high-temperature hydrolysis method.

2 MATERIALS AND METHODS

2.1 Materials

Diethylene glycol (DEG, 99.9 %), anhydrous ferric chloride ($FeCl_3$, 97 %), sodium hydroxide (NaOH, 96 %), and poly acrylic acid (PAA, M_w = 1800) were purchased from the Sigma-Aldrich company. Distilled water was used in all the experiments. All the chemicals were used as received without further treatment and/or purification.

2.2 Synthesis of water-dispersible Fe₃O₄/PAA NPs

The polyol method based on the theory that NPs will be yielded upon heating precursors in a high-boiling-point alcohol at elevated temperature. In this method, DEG is chosen as the solvent because it can easily dissolve a variety of polar inorganic materials due to its high permittivity (ε = 32) and high boiling point (246 °C). DEG is not only a solvent but also a reducing agent in an reaction. Hence, $FeCl_3$ can be used as the only precursor for synthesizing Fe_3O_4. PAA is used as the capping agent, on which the carboxylate groups show a strong coordination with Fe^{3+} on the Fe_3O_4 surface and the uncoordinated carboxylate groups extend into the water solution, rendering the particles with high water dispersibility. A strong coordination of carboxylate groups with the surface iron cations and the multiple anchor points for every single polymer chain is an important factor in creating a robust surface coating of PAA on magnetite NPs. Therefore, we used PAA as the capping agent in our synthesis to confer upon the particles high water dispersibility. A mixture of ethanol and water was used to wash the particles and remove the unwanted leftover material from the particles.

For the synthesis of Fe_3O_4 NPs, a NaOH/DEG solution was prepared by dissolving 100 mmol of NaOH

in 40 ml of DEG at 120 °C under nitrogen for 1h. Then the light-yellow solution was cooled to 70 °C (the stock solution A). In a 100-ml, three-necked flask equipped with a nitrogen inlet, a stirrer and a condenser, 10 mmol of $FeCl_3$ and 20 mmol of PAA were dissolved in 41 ml of DEG under vigorous stirring. The solution was purged with bubbling nitrogen for 1 h and then heated to 220 °C for 50 min (the stock solution B). Subsequently, 20 ml of the NaOH/DEG solution was injected rapidly into the above solution. The reaction was allowed to proceed for 2 h. The black color of the solution confirms the formation of magnetite NPs. The resultant black product was repetitively washed with a mixture of ethanol and water and collected with the help of a magnet. The cycle of washing and magnetic separation was performed five times. A one-pot synthesis was done with the Fe_3O_4/PAA particles, so no extra process was needed for the surface modification. A flow chart of the synthesis is shown in **Figure 1**.

3 CHARACTERIZATION

3.1 Structural and magnetic characterization of Fe₃O₄/PAA NPs

A powder X-ray diffraction (XRD) analysis was performed on a Phillips EXPERT 1830 diffractometer with Cu K_α radiation. The XRD data were collected over the range of 10–80° (2 θ) with a step interval of 0.02° and a preset time of 1.6 s per step at room temperature. Magnetic measurements were carried out using a Lake-Shore 7400 (Lakeshore Cryotronic) vibration sample magnetometer (VSM) at 300 K. Particle sizes of NPs were measured using a Zetasizer 4 Nano S, dynamic light scattering instrument (Malvern, Worcestershire, UK). Light-scattering measurements were carried out with a laser of the wavelength of 633 nm at the 90° scattering angle. FTIR spectra were recorded on a KBr disc on a Perkin Elmer 100 spectrometer.

For the FR experiments we used a Thorlabs model HGR20 2.0 mW/nm laser source, a GMW Electromagnet-Systems model 5403 electromagnet, a Kepco power-supply model BOP 20-5M, a LakeShore model 455 DSP Gaussmeter, a Stanford research systems model SR830 DSP lock-in amplifier, a new focus model 2051 photo detector, an ILX Lightwave model OMM – 6810B optical multimeter and an OMH – 6703B model silicon power head.

3.2 Experimental setup for a magneto-optical characterization

The magneto-optical-measurement setup is shown in **Figure 2**. The measurements of FR were made using an optical arrangement consisting of a He-Ne laser, a polarizer, MR3-2 magneto-optical glass (from Xi'an Aofa Optoelectronics Technology Inc., China) placed in the gap between the two poles of the electromagnet for the
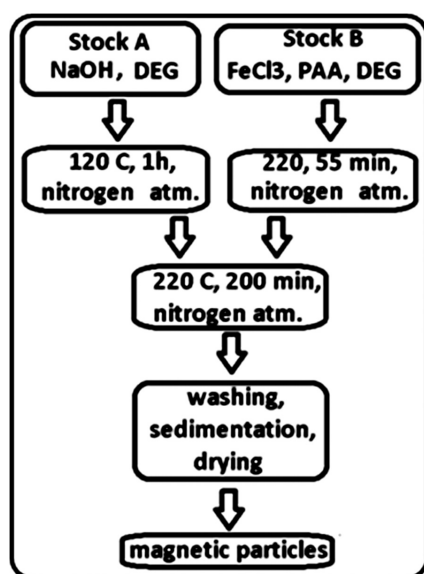

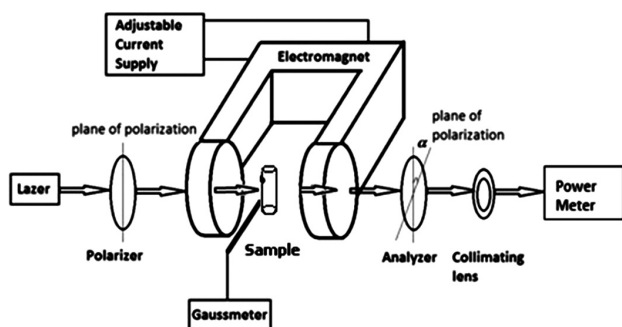**Figure 1:** Flow chart of the synthesis
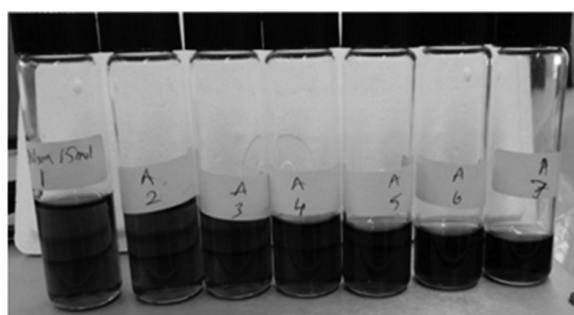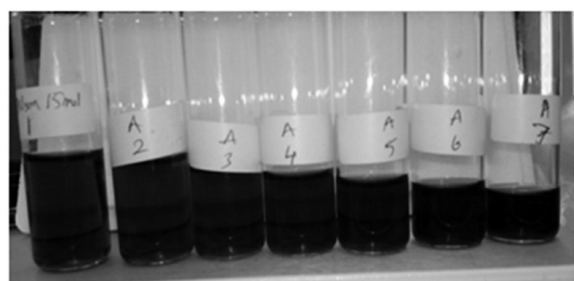**Slika 1:** Potek sinteze

Figure 2: Magneto-optic-measurement setup
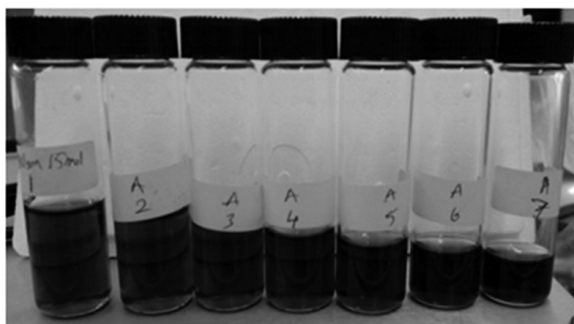**Slika 2:** Magnetooptični merilni sestav

calibration process, an analyzer, collimating lens and a power meter. The electromagnet generates a uniform magnetic field in the sample region. The strength of the

(a)

(b)

(c)

Figure 3: Pictures of the nanofluids containing Fe₃O₄/PAA NPs with various concentrations kept for different times: a) 1 h, b) 2 weeks, c) 4 weeks
Slika 3: Posnetki nanotekočin z Fe₃O₄/PAA-nanodelci z različno koncentracijo po zadržanju: a) 1 h, b) 2 tedna, c) 4 tedne

magnetic field can be adjusted by tuning the magnitude of the supply current and is monitored by a gauss meter.

According to Malus' law, as the polarized light I_0 passes through the transparent magneto-optical material, the light intensity I can be expressed as:

$$l = l_0 \cos^2 \theta = l_0 \cos^2 (\alpha - \phi) \qquad (1)$$

where α is the angle of the polarization axes of the polarizer and analyzer and ϕ is the rotation angle of the polarized plane of the transmitted light. With respect to MFs, this can be expressed as:

$$\phi(B) = C \frac{M(B)}{M_S} VBl(B) \qquad (2)$$

where l is the chain length at the magnetic field B in an MF sample, C is a constant that can be found at a high field assuming that the saturated chain length has no change, M is the magnetization of the sample at the magnetic field B, M_S is the saturation magnetization of the sample and V is the Verdet constant varying with the wavelength and temperature. Generally, a positive Verdet constant corresponds to the L-rotation (anti-clockwise) when the direction of propagation is parallel to the magnetic field and to the R-rotation (clockwise) when the propagation direction is anti-parallel. To obtain the maximum sensitivity of the transmitted power, especially under very small magnetic fields, the FR angle ϕ can be identified as zero and the initial polarization angle of the analyzer is set, with $\alpha = 45°$, according to equation (1). It can be described as:

$$\frac{d(\cos^2(\theta))}{d(\theta)} = 2 \sin \theta \cos \theta = \sin 2\theta \qquad (3)$$

With respect to the FR experiments, the sensitivity is maximum when θ is 45° and $dI/d\Theta = 1$ from equation (3). Therefore, the optical axis of the analyzer is aligned at an angle of 45° to the optical axis of the polarizer.

4 RESULTS

4.1 Stability of Fe₃O₄/PAA-based ferrofluids

NPs in MFs are usually coated with a surfactant material to prevent agglomeration and provide stability.[30–33] The size of a magnetic NP, the material concentration, the carrier liquid and the surfactant are the main variations for MFs.

PAA was selected as a surfactant because of its strong coordination of carboxylate groups with iron cations on a magnetite surface. An additional advantage of PAA is that an extension of the uncoordinated carboxylate groups on polymer chains into an aqueous solution confers on the particles a high degree of dispersibility in water.

A well-dispersed nanofluid was prepared as shown in **Figure 3**. The particle content is 20 mg for various concentrations with an addition of distilled water from 4 ml to 17 ml. NPs can still be dispersing well after the

nanofluid has been kept standing still for more than 4 weeks and no sedimentation is observed for any of the samples. Due to its long-term stability, this kind of MFs is an ideal candidate for optical devices.

4.2 Physical and magnetic properties of Fe$_3$O$_4$/PAA NPs analyzed with XRD, DLS, TEM and FTIR

The crystal structure of the sample was confirmed with an X-ray diffraction (XRD) analysis as shown in **Figure 4**. The (220), (311), (400), (422), (511), and (440) diffraction peaks observed on the curves can be indexed to the cubic spinel structure, and all the peaks were in good agreement with the Fe$_3$O$_4$ phase (JCPDS card 19-0629).

The average diameter of the particles obtained with a dynamic light scattering (DLS) analysis is ~10 nm (**Figure 5**). As seen in the typical transmission electron microscopy (TEM) images of Fe$_3$O$_4$/PAA in **Figure 6a-b**, the average diameter of Fe$_3$O$_4$/PAA was about 8.16 nm **Figure 6c**. The average diameter was obtained by measuring about 100 particles.

The magnetic properties of NPs are shown in **Figure 7** as measured at 300 K with a vibrating sample mag-
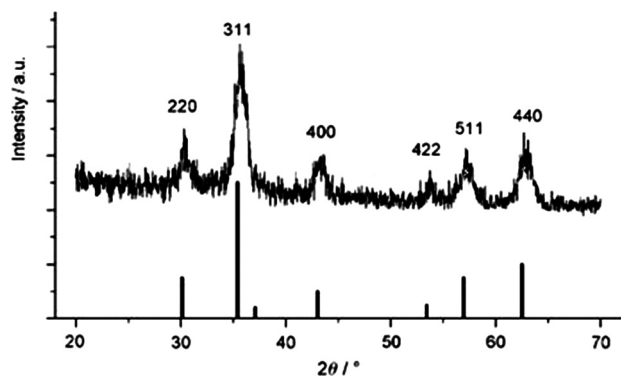

Figure 6: Representative TEM images of magnetite CNCs with: a) 20-nm scale bar, b) 50-nm scale bar, c) the average diameter of Fe$_3$O$_4$/PAA

Slika 6: Reprezentativni TEM-posnetki magnetitnih CNCs: a) merilo 20 nm, b) merilo 50 nm, c) povprečni premer Fe$_3$O$_4$/PAA

Figure 4: X-ray powder-diffraction pattern for PAA-coated Fe$_3$O$_4$ NPs. The peak positions and relative intensities recorded in the literature for bulk Fe$_3$O$_4$ samples are indicated by vertical bars.

Slika 4: Rentgenska difrakcija prahu za s PAA pokritimi Fe$_3$O$_4$-nanodelci. Pozicija vrhov in v literaturi zapisane relativne intenzitete za osnovne Fe$_3$O$_4$-delce so prikazane z navpičnimi črtami.
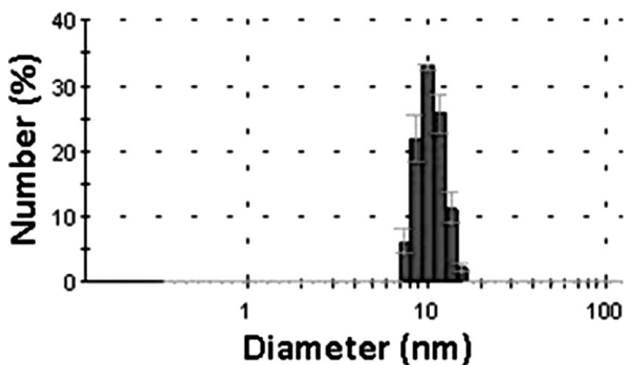

Figure 5: Size distributions of magnetic NPs obtained with DLS
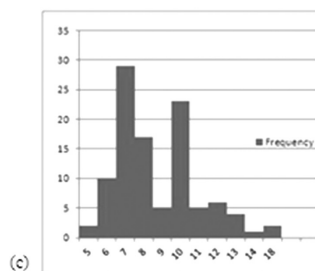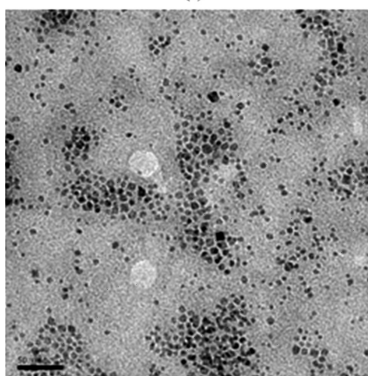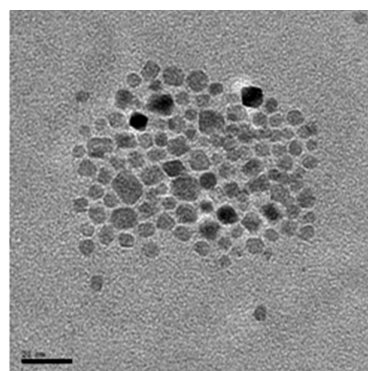**Slika 5:** Razporeditev velikosti magnetnih delcev (NPs), vzeto iz DLS
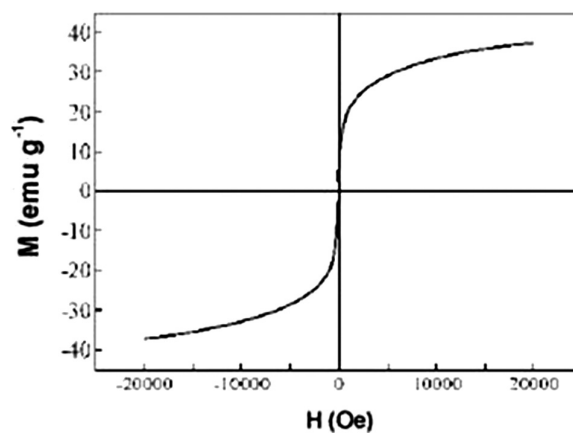

Figure 7: Hysteresis loop of superparamagnetic particles at room temperature
Slika 7: Histerezna zanka superparamagnetnih delcev pri sobni temperaturi
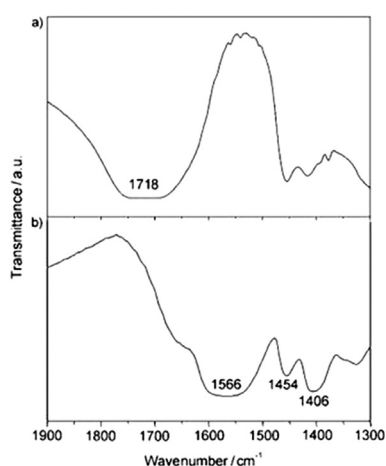
Figure 8: FTIR spectrum of: a) pure PAA, b) PAA with carboxylate-capped Fe₃O₄ NPs
Slika 8: FTIR-spekter: a) čisti PAA, b) PAA s karboksilatom omejeni Fe₃O₄-nanodelci

Figure 9: Applied magnetic-field dependence and concentration dependence of FR
Slika 9: Odvisnost FR od uporabljenega magnetnega polja in koncentracije

netometer (VSM). The saturation magnetization was determined as 38.8 emu/g. The particles showed no remanence or coercivity at 300 K, that is, superparamagnetic behavior.

The stability of PAA capped on Fe₃O₄ was confirmed by measuring the Fourier transform infrared spectroscopy (FTIR) spectrum on the sample as shown in **Figure 8a**. There is a very strong band at around 1718 cm⁻¹ of pure PAA, which is characteristic of the C=O stretching mode for protonated carboxylate groups. The three peaks shown in **Figure 8b** and located at (1566, 1454 and 1406) cm⁻¹ can be assigned to the characteristic bands of the carboxylate (COO⁻) groups, corresponding to the CH₂ bending mode, asymmetric and symmetric C–O stretching modes of the COO⁻ group, respectively.

4.3 Magneto-optic properties of the Fe3O4/PAA-based magnetic fluid

Figure 9 shows FR versus the magnetic field and **Table 1** indicates the maximum rotations of MFs with different concentrations. The field and concentration dependence of FR in MFs was investigated. A 10-mm-thick cuvette was filled with the liquid of 14 various concentrations from 1.8 mg/ml to 5 mg/ml. It can be seen that the rotation increases rapidly with the field at low fields.

The initial susceptibility χ is determined by a linear magnetic response $M = \chi \cdot H$ at the field strength $H \rightarrow 0$ and it depends on the particle concentration of fluids. At low fields in **Figure 9** the initial slope is:

$$m_i = \frac{C}{B} \frac{M(B)}{M_s} + Vl(B) \qquad (4)$$

As long as the concentration is decreased, fewer NPs are found in the medium and this situation causes a lower magnetization and a shorter chain length at a
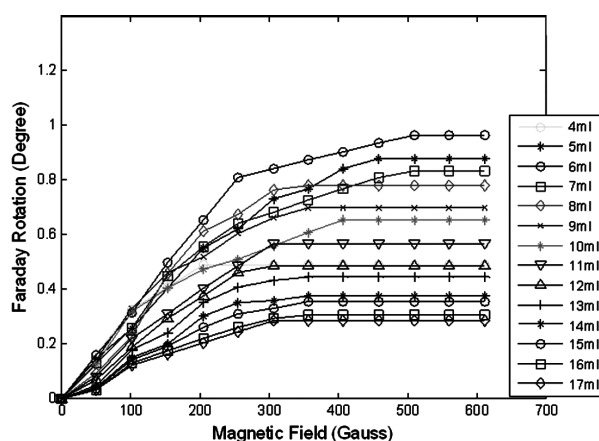
particular field. In other words, the volume fraction of MF and the initial slope are decreased. Black curves relate to samples 8–14 (**Table 1**) and their slopes are less steep than the ones of the first seven samples, because their magnetizations are lower and the chain lengths are shorter than those of the first seven samples. It needs to be pointed out that though the maximum FR of sample 1 (indicated as the yellow curve) is relatively low, its initial susceptibility is the highest value due to the volume fraction.

Table 1: Maximum FRs of the samples with different concentrations
Tabela 1: Maksimalna Faradayeva rotacija (FR) pri vzorcih z različnimi koncentracijami

Sample	Particle	Water	Concentration	Faraday rot.
no	mg	ml	mg/ml	Max. degree
1	20	4	5.00	0.49
2	20	5	4.00	0.87
3	20	6	3.33 ($C_{CRITICAL}$)	0.96
4	20	7	2.86	0.83
5	20	8	2.50	0.78
6	20	9	2.22	0.70
7	20	10	2.00	0.65
8	20	11	1.82	0.56
9	20	12	1.67	0.48
10	20	13	1.54	0.44
11	20	14	1.43	0.37
12	20	15	1.33	0.35
13	20	16	1.25	0.30
14	20	17	1.18	0.28

As the volume fraction of NPs increases, dipole interactions between the particles overcome the thermal forces more easily. A graphical representation of the maximum FR can be seen in **Figure 10**. It is important to mention that most experimental investigations, based on optical observations, of the chain formation in MFs are usually carried out on the samples in the low concentration regime, where the chain-chain interaction is weak.
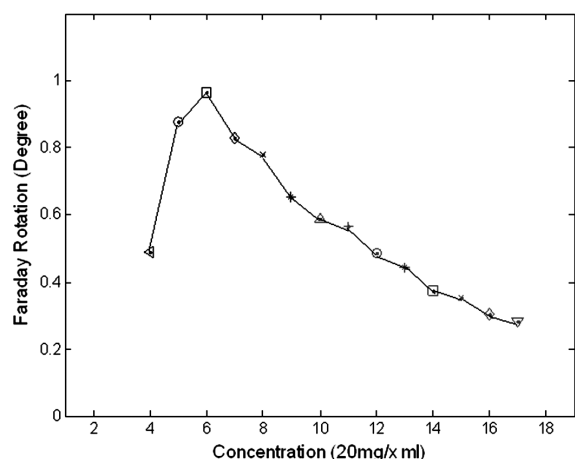
Figure 10: Graph of the maximum FR of the samples
Slika 10: Graf maksimalne Faradayeve rotacije (FR) vzorcev

However, we tried many samples with variable concentrations to see the effect of higher concentrations. When we analyze **Figure 10**, it can be seen that FR increases with higher concentrations (from 1.18 mg/ml to 2.26 mg/ml) up to $C_{CRITICAL}$ (3.33 mg/ml). But after the $C_{CRITICAL}$ (sample 3) value, FR tends to decrease with higher concentrations (4 mg/ml and 5 mg/ml). According
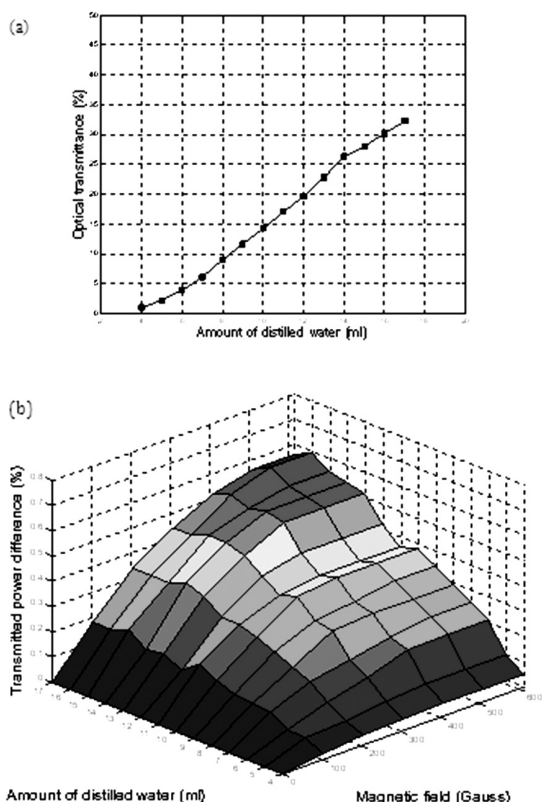

Figure 11: a) Transmissivity of Fe₃O₄ NPs, $B = 0$ T, b) transmitted power difference of Fe₃O₄ NPs at particular fields and with different concentrations
Slika 11: a) Transmisivnost Fe₃O₄-nanodelcev, $B = 0$ T, b) posredovana razlika v moči Fe₃O₄-nano delcev pri določenem polju z različno koncentracijo

to Stokes' law, there is a friction between the moving particles and the carrier fluids, which depends on the viscosity of the fluids.[34] Thus, the viscosity of MF and the friction in the medium were high for highly concentrated MFs and they affected the activity of the magnetic particles. It is also important to point out that the chain-chain interaction becomes much stronger once the concentration of a sample is increased and may lead to the closure of some chains or even the curling.[35,36] Therefore, it can be said that FR tends to decrease after $C_{CRITICAL}$ due to the substructure (particle-particle, chain-chain) interactions.

Figure 11a shows the transmission of unpolarized light as percentage and **Figure 11b** shows the transmission difference of unpolarized light under magnetic fields for each concentration in the $1–6 \cdot 10^{-2}$ T region. The transmitted light difference as percentage in **Figure 12b** is calculated from the difference between the intensity of the light transmitted in a particular ($1–6 \cdot 10^{-2}$ T) magnetic field and the intensity in the zero field for the samples with different concentrations.

Low transmission responses to magnetic fields were observed for samples 1 and 2. Except for these samples, remarkable changes were observed for all the other samples because of the weakening of the viscosity effect. It can be said that samples 1 and 2 have a blocking property and other samples have a channeling property due to their concentrations. A decreasing percentage of NPs in a unit volume indicates a lower magnetization and a smaller chain length, which play important roles in the Faraday effect.[37]

5 DISCUSSION

5.1 Model for Explaining the Experimental Results

There are two physical phenomena for the magneto-optical effect in MFs in the presence of an external magnetic field. One is the orientation theory (magnetic orientation or physical orientation) based on the optical anisotropy of magnetic particles or its aggregation, and the other is the formation theory based on the chain formation of the magnetic particles (**Figure 12**). In the zero magnetic field the particles are distributed randomly with
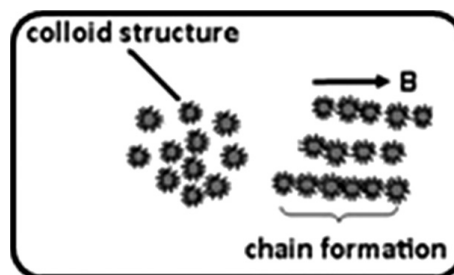

Figure 12: Magnetic NP alignment and the chain formation in the direction of the external magnetic field
Slika 12: Magnetna ureditev nanodelcev in nastajanje verig v smeri zunanjega magnetnega polja

no coercivity and remanence forming an isotropic material. Particles start to coagulate and form chain-like structures in the direction of the field with the help of an external magnetic field.[38,39]

Magnetic field induces NPs to line up or to behave asymmetrically, introducing anisotropy and resulting in birefringence. If lattice atoms of a crystal were not completely symmetrically arrayed, the binding forces on the electrons would be anisotropic, causing a material to be circularly birefringent with different indices of refraction.[40] When the applied magnetic field's direction is parallel to the light beam, the anisotropy is circular in a longitudinal configuration. However, the rotation of polarization does not seem to be linked to the particles' anisotropy-axis orientation but to the orientation of the magnetic moments of the particles in the applied field's (H) direction.[41]

When an external magnetic field is applied parallel to the plane of MF, magnetic particles in the fluid agglomerate to form chain-like structures. As the field strength is further increased, more particles contribute to agglomeration and the chains become longer under a higher field. It has been found that the chain length varies with the applied magnetic field and with the concentration of the MF.[42] In some experimental conditions, in which the wavelength of the electromagnetic waves passed through the sample is very small in comparison with the chain length, FR is not only governed by magnetization of the fluid but also affected by the chain formation.[43]

Additionally, MFs can be diluted magnetically by passive liquid carriers such as glycerol, ethylene glycol, diester, isopar M, ethanol or simply distilled water and it was seen that FR was affected by a change in the concentration. Different concentrations of MFs can help us describe various friction forces among the magnetic NPs. Carrier fluids significantly influence the response of the Faraday effect. Consequently, the chain formation is a crucial parameter of the optical properties of MFs. The chain lengths in MFs composed of magnetic NPs vary with respect to concentration.[44–46]

The positional and magnetic field dependence of the colloidal assembly of magnetite NPs arise from a sensitive interplay between the local concentrations of the particles, causing the effect of three types of forces between the colloidal NPs. These forces are (1) the hard-sphere repulsion between the particles in contact; (2) a combination of electrostatic repulsion due to the presence of the charges on the surface of NPs and Van-der-Waals attraction; (3) the magnetic dipolar attraction/repulsion due to the magnetite cores of the particles. The interaction potential of the third force is given by:

$$U_{ab}(r) = \frac{1}{r^2}(\vec{\mu}_a \cdot \vec{\mu}_b) \qquad (5)$$

The dipolar interaction between two magnetic particles, a and b, depends on the magnitude and direction of their magnetic moments μ_i as well as on their relative position r_{ab}. Depending on the particles configuration, the dipolar energy may be repulsive or attractive. Heinrich and coworkers showed that these forces play a role in the assembly of magnetic nano-particles.[47] When a magnetic field is applied these particles initially form chain-like structures. These chains are then arranged into two-dimensional hexagonally packed sheets. This occurs by shifting a neighboring chain by a distance of r corresponding to the radius of NP. The chains are formed along the direction of an external magnetic field.

6 CONCLUSION

In conclusion, high-quality Fe₃O₄/PAA-based nanostructures for MF formation were synthesized successfully and FR investigations were made for many samples with variable concentrations. We report the first demonstration of FR for MF synthesized with this novel method. We have demonstrated the FR of a highly water-soluble MF that was measured to be in the 0–6 · 10⁻² T range in the DC regime. The effects of both viscosity and chain formation were observed on FR. We found the maximum FR to be 0.96°/(10 mm) at room temperature for 3.33 mg/ml. FR was on an increase with the higher concentrations up to $C_{CRITICAL}$. It was found that the rotation begins to decrease again when the concentration is higher than $C_{CRITICAL}$. The reason for this might be the blocking effect that arises from the particle-particle and chain-chain interactions. The experiment results shed some light on the role of agglomeration and chain formation in FR. Taking into account the flexibility of the liquid form (including the long-term stability and no-sedimentation property) in order to predict its optical behavior correctly, and the low-magnetic-field requirements, these fluids can be exploited for the fabrication of a wide range of applications in magneto-optics.

7 REFERENCES

[1] J. Ge, Y. Hu, Y. Yin, Angew. Chem. Int. Ed., 46 (**2007**), 7428–7432

[2] P. H. C. Camargo, Z. Y. Li, Y. Xia, Soft Matter, 3 (**2007**), 1215–1222

[3] K. Butter, P. H. H. Bomans, P. M. Frederik, G. J. Vroege, A. P. Philipse, Nature Materials, 2 (**2003**), 88–91

[4] A. Yethiraj, A. van Blaaderen, Nature, 421 (**2003**), 513–517

[5] M. Klokkenburg, C. Vonk, E. M. Claesson, J. D. Meeldijk, B. H. Erne, A. P. Philipse, J. Am. Chem. Soc., 51 (**2004**), 16706–16707

[6] A. P. Hynninen, M. Dijkstra, Phys. Rev. Lett., 94 (**2005**), 138303

[7] M. Klokkenburg, B. H. Erne, J. D. Meeldijk, A. Widenmann, A. V. Petukhov, R. P. A. Dullens, A. P. Philipse, Phys. Rev. Lett., 9 (**2006**), 185702

[8] A. K. Agarwal, A. Yethiraj,. Phys. Rev. Lett., 102 (**2000**), 198301

[9] T. J. Yoon, K. N. Yu, E. Kim, J. S. Kim, B. G. Kim, S. H. Yun, B. H. Sohn, M. H. Cho, J. K. Lee, S. B. Park, Small 2 (**2006**) 2, 209–215

[10] J. Lee, Y. Lee, J. K. Youn, H. B. Na, T. Yu, H. Kim, S. M. Lee, Y. M. Koo, J. H. Kwak, H. G. Park, H. N. Chang, M. Hwang, J. G. Park, J. Kim, T. Hyeon, Small 4 (**2008**) 1, 143–152

[11] J. H. Lee, Y. M. Huh, Y. W. Jun, J. W. Seo, J. T. Jang, H. T. Song, S. Kim, E. J. Cho, H. G. Yoon, J. S. Suh, J. Cheon, Nature Medicine, 13 (**2007**) 1, 95–99

[12] J. H. Lee, K. Lee, S. H. Moon, Y. Lee, T. Gwan Park, J. Cheon, All-in-One Target-Cell-Specific, Angew. Chem. Int. Ed., 48 (**2009**), 4174–4179

[13] C. Xu, K. Xu, H. Gu, X. Zhong, Z. Guo, R. Zheng, X. Zhang, B. J. Xu, Am. Chem. Soc., 126 (**2004**), 3392–3393

[14] A. H. Lu, E. L. Salabas, F. Schuth, Angew. Chem. Int. Ed., 46 (**2007**), 1222–1244

[15] X. Zhao, R. Tapec-Dytioco, K. Wang, W. Tan, Anal. Chem., 75 (**2003**), 3476

[16] S. V. Sonti, A. Bose, Colloids and Surfaces B-Biointerfaces, 8 (**1997**) 4–5, 199–204

[17] S. Liu, E. Li, Q. Zhou, IEEE 3rd Int. Conf. on Bio. Eng. and Inf., (**2010**), 1532–1535

[18] S. Pu, M. Dai, G. Sun, Opt. Comm., 283 (**2010**), 4012–4016

[19] C. Y. Hong, J. Mag. Mag. Mat., 201 (**1999**), 178–181

[20] L. Martinez, F. Cecelja, R. Rakowski, Sens. Act. A, 123–124 (**2005**), 438–443

[21] J. Ge, Y. Hu, M. Biasini, W. P. Beyermann, Y. Yin, Angew. Chem. Int. Ed., 46 (**2007**) 23, 4342–4345

[22] N. A. Yusuf, J. Appl. Phys., 64 (**1988**), 5

[23] Z. D. Xianfeng, Appl. Phys. Lett., 89 (**2006**), 211106

[24] Y. T. Pan, J. Appl. Phys., 73 (**1993**), 10

[25] X. Fang, Nanoscale Research Letters, 6 (**2011**), 237

[26] M. M. Maiorov, J. Magnetism and Magnetic materials, 252 (**2002**), 111–113

[27] F. Royera, D. Jamona, J. J. Rousseaua, V. Cabuila, D. Zinsa, H. Rouxa, C. Boviera, The European Physical Journal Applied Physic, 22 (**2003**) 2, 83–87

[28] N. A. Yusuf, A. A. Rousan, H. M. El-Ghanem, J. Appl. Phys., 64 (**1988**), 2781

[29] N. A. Yusuf, I. Abu-Aljarayesh, A. A. Rousan, H. M. El-Ghanem, IEEE Trans. on Magn., 26 (**1990**), 5

[30] R. E. Rosensweig, Nature, 210 (**1966**), 613

[31] M. I. Shliomis, Zh. Eksp. Teor. Fiz., 61 (**1971**), 2411

[32] D. H. Lee, R. A. Condrate, J. S. Reed, J. Mater. Sci., 31 (**1996**), 471

[33] H. Li, C. P. Tripp, Langmuir, 21 (**2005**), 2585

[34] D. Lin, W. Shibin, L. Sen, IEEE Ann. Rep. Conf. on El. Ins. and Diel. Pheno., 2010

[35] P. C. Scholten, IEEE Trans. Magn., 16 (**1980**), 221

[36] P. G. De Gennes, P. A. Pincus, Phys. Condens. Matter, 11 (**1990**), 189

[37] R. E. Rosensweig, Magnetic Fluids, Annual Reviews

[38] M. Wu, Y. Xiong, Y. Jia, H. Niu, H. Qi, J. Ye, Q. Chen, Chem. Phy. Lett., 401 (**2005**), 374–379

[39] H. E. Horng, C. Y. Hong, S. Y. Yang, H. C. Yang, J. Phy. and Chem. of Sol., 62 (**2001**), 1749–1764

[40] E. Hecht, Optics, 4ᵗʰ ed., Addison Wesley

[41] F. Royer, D. Jamon, J. J. Rousseau, V. Cabuil, D. Zins, H. Roux, C. Bovier, Eur. Phys. J. AP, 22 (**2003**), 83–87

[42] N. A. Yusuf, J. Phys. D: Appl. Phys., 22 (**1989**), 1916–1919

[43] A. A. Rousan, H. M. El-Ghanem, N. A. Yusuf, IEEE Trans. on Mag., 25 (**1989**) 4, 3121–3124

[44] N. A. Yusuf, I. Abu-Aljarayesh, A. A. Rousan, H. M. El-Ghanem, IEEE Trans. on Mag., 26 (**1990**) 5, 2852–2855

[45] G. A. Jones, H. Niedoba, J. of Mag. and Mag. Mat., 73 (**1988**), 33

[46] W. Syed, D. A. Hammer, M. Lipson, Opt. Let., 34 (**2009**) 7, 1009–1011

[47] D. Heinrich, A. R. Goni, A. Smessaert, S. H. L. Klapp, L. M. C. Cerioni, T. M. Osan, D. J. Pusiol, C. Thomsen, Phys. Rev. Lett., 106 (**2011**), 208301